Available online at www.sciencedirect.com
ScienceDirect
Advances in Space Research 38 (2006) 173–179
ADVANCES IN SPACE RESEARCH (a COSPAR publication)
www.elsevier.com/locate/asr

Dst of the Carrington storm of 1859

G. Siscoe [a,*], N.U. Crooker [a], C.R. Clauer [b]

[a] Center for Space Physics, Boston University, 725 Commonwealth Avenue, Boston, MA 02215, USA
[b] Space Research Laboratory, University of Michigan, 2455 Hayward, Ann Arbor, MI 48109-2143, USA

Received 29 December 2004; received in revised form 21 February 2005; accepted 24 February 2005

Abstract

The super-storm of 1859 gives an opportunity to apply models to predict Dst that have been exercised mostly on non-extreme cases. The exercise gains significance through a Bombay magnetogram that Tsurutani et al. (2003) recently published showing a negative H excursion of ~1600 nT, which is unprecedented for the latitude of the station, and which presents difficulties of interpretation if the negative excursion is taken to be equivalent to Dst. Following a suggestion by Li et al. (2005), we have replaced the original Bombay magnetogram, which has many points per hour during the interesting phase of the storm, by hourly averages, thereby constructing a time profile that is closer to a Dst profile as it is usually calculated. Then, the maximum H-depression is ~−850 nT, which lies not so astonishingly outside the officially observed range. The Bombay magnetogram exhibits two major H-depressions, which we interpret to mean that the event was caused by a geoeffective ICME-sheath followed by a magnetic cloud across which the magnetic field rotated from north to south. On this interpretation, the ICME-sheath caused the extraordinary −1600 nT excursion in H. Then, the issue is whether this large excursion was produced by ionospheric currents (in which case it is not so exceptional) or by magnetospheric currents (in which case it is unprecedented)? To explore the second possibility, we use empirical models that relate the measured shock transit time to the ICME speed and peak magnetic field strength at 1 AU together with average pre-shock interplanetary conditions to construct geoeffective parameters throughout the ICME-sheath. We use the Burton et al. equation as modified by O'Brien and McPherron to calculate Dst. The resulting Dst profile lies reasonably close to hourly averaged Bombay magnetogram, especially if one uses the upper limit allowed for field strength in the ICME-sheath or if one discards the most extreme outlier of the Bombay measurements. We conclude that it is possible to interpret the Bombay magnetogram as having been produced by the magnetospheric currents.

Keywords: 1859 storm; Carrington; Super-storms

1. Purpose of modeling the 1859 storm

The Carrington storm of 1859 provides a useful test case on which to exercise models that relate ICME parameters to shock transit time and that predict associated magnetospheric effects. Because there are so few measurements to work with, however, it is unrealistic to expect the exercise to be definitive. Indeed, the basic data on the event are merely its position in the series of sunspot cycles (the rising phase of cycle 10), the location on the sun of the associated flare (20° N, 15° E), and the shock transit time (~17.6 h) (both given in Carrington, 1860, but see below for a revision of the shock transit time), the information that the storm produced auroras seen overhead in Florida at magnetic latitude of 37° (Loomis, 1866), and a magnetogram from Bombay, India, that has been recently calibrated (shown below) (Tsurutani et al., 2003).

By itself, the shock transit time, from which one can infer the speed of the ICME at earth, is an unreliable predictor of the intensity of a magnetic storm. For example, the fastest ICME on record (flare-to-SSC transit time of 14.6 h, August 4, 1972) produced a storm of relative modest intensity as measured by Dst (−125 nT), whereas by the same measure a rather slow ICME on 13 March 1989 (flare-to-SSC transit time of 54.8 h – 3.8 times longer than the shortest time just mentioned) produced the most intense super-storm on record (Dst = −589 nT) (Cliver

* Corresponding author. Tel.: +1 617 353 5990; fax: +1 617 353 6463.
E-mail address: siscoe@bu.edu (G. Siscoe).

0273-1177/$30 © 2006 Published by Elsevier Ltd on behalf of COSPAR.
doi:10.1016/j.asr.2005.02.102

et al., 1990, 1992). Obviously, therefore, the ICME speed, which can be inferred from the shock transit time, must be supplemented with information on the IMF to predict even the category – small, moderate, major, or super – into which a storm will fall.

Regarding supplemental information on the IMF for the 1859 storm, we know only that during even-numbered sunspot cycles (into which 1859 fell) there is a statistical tendency for the IMF to rotate from northward to southward through the magnetic clouds of ICMEs (Bothmer and Rust, 1997; Mulligan et al., 1998). Nonetheless, the fact that the 1859 storm produced auroras seen overhead in Florida means that it fell in the super-storm category, which, despite the lack of direct measurements, means that the IMF must have pointed southward for a sufficient time. But whether the IMF depressed Dst as far as it could have done, by pointing straight south, or only partially, we cannot say by direct measurement.

We can, however, determine the maximum Dst that empirical models predict for the 1859 ICME, and this determination is the value of the exercise. The exercise also bears on an ambiguity regarding the interpretation of the Bombay magnetogram (Fig. 1). We proceed, therefore, by subjecting the 1859 event to an idealized, "textbook" analysis using only climatological (and therefore unbiased) values for quantities not determined by models. Under this constraint of unbiased input parameters, the intention is to set up the analysis so as to maximize the effects of the Carrington ICME and thereby to calculate how severe, according to the models, it could have been, especially as measured by Dst.

2. Connection between the Bombay magnetogram and Dst

The Bombay magnetogram shown in Fig. 1 has played an important role in rekindling interest in the 1859 storm. On the basis of this magnetogram, Tsurutani et al. (2003) concluded that Dst dropped to the extraordinary value of

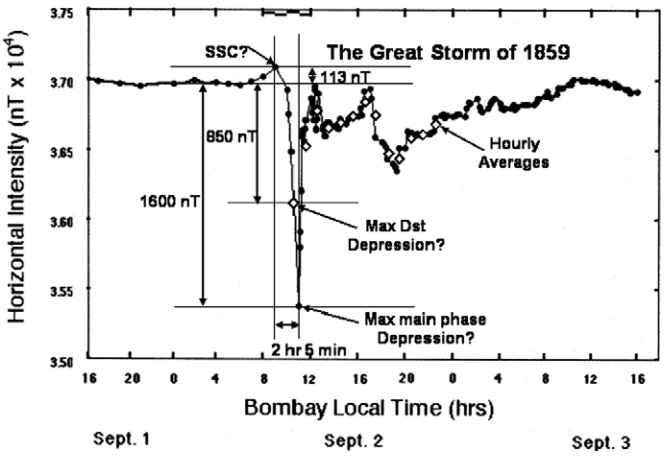

Fig. 1. Magnetogram of the horizontal geomagnetic field intensity from Bombay, India, covering the magnetic storm of September 2, 1859. Modified from Tsurutani et al. (2003).

−1760 nT, which if true, would be nearly three times lower than the great storm of March 1989, which, as previously noted, reached a Dst of −589 nT (Cliver et al., 1992). For the 1859 storm, Loomis (1866) cites magnetic disturbances at other magnetic observatories as being either off scale or between 1/30th and 1/8th of the mean horizontal strength, which corresponds roughly to 1000–3000 nT. But these observatories were at high magnetic latitudes or in the case of Rome, Italy, reported overhead auroras, so it is likely that the cause of the unusually strong magnetic disturbance in these cases was ionospheric current rather than the ring current, which governs Dst. Probably an upper limit on the depth of the 1859 Dst depression is around −950 nT, which Siscoe (1979) found by extrapolating to 37° (the latitude in Florida at which an aurora was seen overhead) a plot of the lower latitudinal limit of quiet auroral arcs versus Dst that Akasofu and Chapman (1963) compiled using IGY data. This extrapolation of their result to 37° should be an upper limit for the 1859 Dst depression because the Akasofu and Chapman compilation refers to discrete arcs visible in IGY all sky cameras, whereas the aurora seen overhead in 1859 in Florida might have been a sub-auroral red arc (Silverman, 2005, this issue) at a latitude lower than discrete arcs.

The southernmost appearance of the aurora in the United States coincided very nearly with the maximum drop in the H component around 11 a.m., local Bombay time seen in the Bombay magnetogram (Loomis, 1866). At this same time the magnetometer at the astronomical observatory in Rome, Italy, registered an unprecedented horizontal field excursion of nearly 3000 nT (Loomis, 1860, p. 397). These supplementary pieces of information indicate that the deep excursion of H seen in the Bombay magnetogram between 9 and 12 h local time indeed marks the peak of storm intensity for the entire storm, which continued until September 4.

Fig. 1 shows the Bombay magnetogram of the 1859 magnetic storm presented by Tsurutani et al. (2003) with lines added to mark extremes of field excursions. Diamond symbols were also added that give hourly averages. Hourly averages, as Li et al. (2005) point out in connection with this magnetogram, better represent Dst, which is normally taken to be an hourly index. The hourly average diamonds begin at 10 a.m. on Sept. 2nd when the cadence of recording changed from the standard (for the time) one measurement per hour to a faster rate evidently instituted in response to the advent of the storm. They end 14 h later after the difference between hourly averages and actual measurements becomes unimportant for the purpose of modeling.

Besides taking hourly averages as a step toward bringing the Bombay magnetogram closer to a representation of Dst, one must also consider a possible correction for the disturbance field asymmetry, which during major magnetic storms can be comparable to Dst itself. For example, the H value that the magnetometer recorded when the storm peaked might have been, say, 50% higher or lower than the actual Dst or anywhere in between depending on the local-time phase of the asymmetry relative to the local time

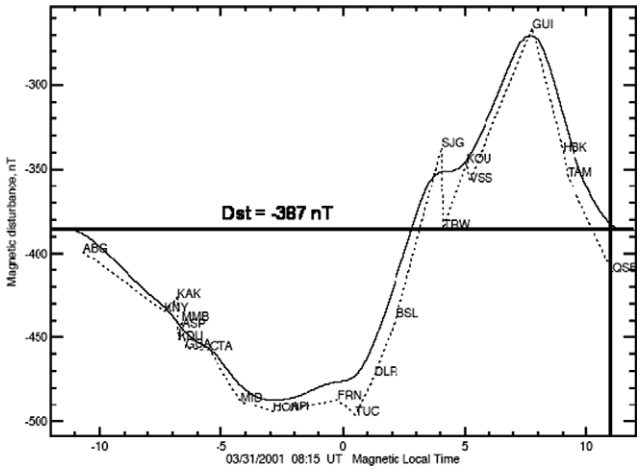

Fig. 2. The H component of the disturbance field measured at 23 low-latitude observatories at the peal of the magnetic storm of March 31, 2001. The solid line is a smooth fit to the points. The thick horizontal and vertical lines mark Dst at this time and the local time of Bombay at the peak of the 1859 storm. They cross at the observed value of the H component.

of Bombay (~11:00). Fig. 2 illustrates the point for the major magnetic storm of March 31, 2001. The plot shows the H component measured at 23 low-latitude stations, well distributed in longitude, at the peak of the storm. Values vary from about −270 to about −490 nT, the average being very close to the official Dst at this time (−387 nT). Note that the value at 11:00 h local time (where Bombay was at the peak of the 1859 storm) is nearly identical with Dst.

This rather fortuitous circumstance – that the value of the H component of the disturbance field at 11:00 h local time happens approximately to equal Dst – seems to be a general rule for major magnetic storms as shown in Table 1. Here, the values of the H component of the disturbance field at 11:00 h local time are compared with Dst at peaks of nine magnetic storms. (The Oct. 30, 2003 storm appears twice as it had two main phases.) In most cases H and Dst differ by less than 20 nT. The last two entries in the table show the biggest differences. In one case, Dst is 71 nT more negative than H, in the other 58 nT more positive. The averages are nearly equal. As far as the disturbance field asymmetry is concerned, therefore, the value of the Bombay magnetogram at the peak of the 1859 storm can be taken as a reasonable proxy for Dst.

Table 1
A comparison of the peak Dst values for nine recent major magnetic storms and the corresponding values of the H component of the disturbance magnetic field at 11:00 h local time (the local time of Bombay at the peak of the 11859 storm)

Date and time	Dst (nT)	H (nT) at 11 h LT
March 25, 1991, 01:5 UT	−293	−280
Nov. 9, 1991, 01:31 UT	−354	−335
May 10, 1992, 12:05 UT	−266	−270
April 7, 2000, 00:09	−288	−290
July 15, 2000, 21:55	−289	−290
March 31, 2001, 08:15	−387	−387
Oct. 30, 2003, 00:30	−363	−390
Oct 30, 2003, 22:30	−401	−320
Nov. 20, 2003, 19:10	−472	−530
Average	−346	−344

3. Interpretation and set up

We think that the simplest interpretation of the Bombay magnetogram is that it shows a storm with two main phases, which happens for more than 50% of intense magnetic storms (Kamide et al., 1998), the first of which, lasting approximately between 09:00 and 11:00 h on Sept. 2nd, was driven by the ICME-sheath (the region between the ICME shock wave and the ICME body) and the second main phase, lasting approximately between 17:00 and 19:00 h, being driven by the trailing half of the ICME body. Regarding the global nature of the second phase of the storm, we note that on Sept. 2nd the vertical magnetic field component at the Rome observatory mentioned above went off scale just when the second phase seen in the Bombay magnetogram peaked (19 h local Bombay time, Loomis, 1860, p. 397). This two-main-phase interpretation implies a southward IMF in the ICME-sheath followed by a north-then-south rotation of the IMF as the ICME cloud swept over the earth, which is consistent with the statistical expectation for even-numbered sunspot cycles. Our interpretation differs from that preferred by Tsurutani et al. (2003) who think that the storm was driven not by the ICME-sheath, which they assume lasted only about 1 h and had little effect, but by the leading half of the ICME body, which they assume also lasted about 1 h.

The primary solar wind parameter that we shall use to calculate Dst is the interplanetary electric field ($E = -V \times B$). To specify E for the 1859 storm, we assume that the ICME hit the earth dead-on, which means that in the ICME frame of reference the earth moved through the ICME-sheath from the ICME bow shock to the ICME-pause along the ICME stagnation stream line. We then apply to the following models: maximum speed of the ICME driver gas ($V_{\max}$, presumably the leading edge of the ICME itself) versus average shock transit speed ($\langle V_{\rm shk}\rangle$) (Cliver et al., 1990):

$$V_{\max} = 0.775\langle V_{\rm shk}\rangle - 40\ \text{km/s}. \quad (1)$$

This formula gives a value very close to 1900 km/s for $V_{\max}$. By analogy to planetary magnetospheres where, for steady solar wind conditions, a standing bow shock sits at a fixed distance in front of the magnetopause, we assume that the ICME bow shock and the leading edge of the ICME move at the same speed (1900 km/s at 1 AU). For pre-shock solar wind and IMF parameters, we use climatology (i.e., values that typify the ordinary solar wind): $V = 400$ km/s, $n = 5/\text{cm}^3$, and $B = 5$ nT. To maximize the geoeffectiveness of the storm, we point the IMF straight south throughout the ICME-sheath. Post-shock solar wind and IMF parameters we determine by the strong shock jump conditions applied to the pre-shock values (in the shock frame of reference these are a factor of 4 jump in

density, field strength, and inverse velocity). These give post-shock values of 20/cm^3, 20 nT, and 1523 km/s after adding the shock speed to convert to earth's reference frame. Based on MHD simulations for earth's magnetosheath (Siscoe et al., 2002), density remains approximately constant between the shock and the leading edge of the ICME (ignoring here the so-called depletion layer), and velocity rises linearly from its post-shock value in the earth's reference frame to that of the leading edge of the ICME.

To specify the variation of the magnetic field strength from its post-shock, factor-of-four jump to its value at the leading edge of the ICME, we again appeal to MHD simulations of earth's magnetosheath. Fig. 3 shows magnetic field strength along the stagnation stream line in earth magnetosheath and adjacent regions for MHD simulations of five IMF orientations (clock angles 0°, 45°, 90°, 135°, and 180°), as indicated in the figure. Horizontal lines mark special values of field strength: the pre-shock value (5 nT), the post-shock value (~20 nT), the 'merging' value (~32 nT, explained below), and the stagnation value (~50 nT). All are self-explanatory except the 'merging' value, which, as the figure indicates, is the peak sheath value attained when the IMF has a non-northward component (the clock angle = 90°, 135°, and 180° cases), and so, presumably corresponds to an upper limit set by dayside, subsolar merging. Its value agrees with an empirical formula found by Crooker et al. (1982): two times the geometric mean of the transverse component of the IMF and the stagnation field strength. The important point for the present application is that the sheath portions of all five curves are self-similar in that if they are translated and stretched to make their beginning and end points match, the curves nearly coincide. Thus, a single formula appears to fit the five curves reasonably well:

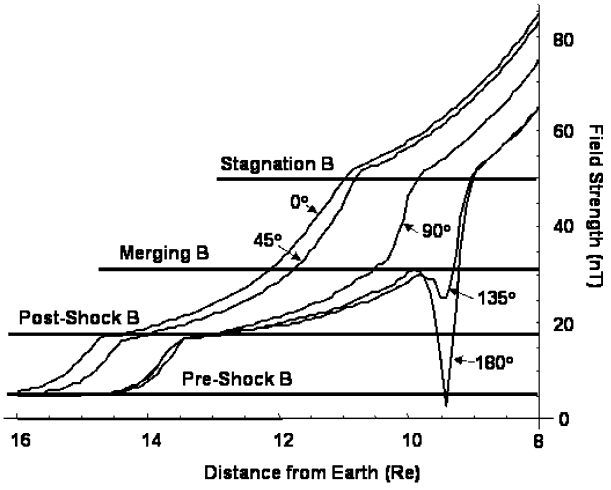

Fig. 3. Magnetic field strength along the stagnation streamline in earth's magnetosheath for five IMF orientations, as indicated by clock angles. (Computed with the ISM MHD code, White et al., 2001) (Wiggles in the lines are, of course, artificial and result from connecting values interpolated at discrete distances between grid points.)

$$B_{\rm sh}(\xi) = B1 + (B2 - B1)(-0.008164 + 0.41054\xi - 0.32648\xi^2 + 0.91752\xi^3), \quad (2)$$

where $B1$ is the post-shock field strength, $B2$ is the field strength at the magnetopause, and ξ is the normalized distance between the shock and the magnetopause measured earthward from the shock.

$$\xi = (x(\text{shock}) - x)/(x(\text{shock}) - x(\text{m'pause})). \quad (3)$$

Although this formula was obtained from simulations of earth's magnetosheath, we use it also to specify the field strength in the magnetosheath of the ICME, for several such algorithms we have considered (e.g., Lees, 1964), none has more physical justification.

To apply Eq. (2) to the magnetosheath of the 1859 ICME, we need to specify only $B2$, the value of the magnetic field strength at the leading edge of the ICME, since, as already noted, we assume that $B1 = 20$ nT. To specify $B2$, we use an empirical relation derived by Owens and Cargill (2004) for the peak field strength in ICME-sheaths, which we take to be the value that applies at the leading edge of the ICME body:

$$\text{peak}\, B_{\rm sh} = 0.08(V_{\max} - V_{\rm SW}) + 12.12\ \text{nT}, \quad (4)$$

where $V_{\rm SW}$ is the speed of the solar wind ahead of the ICME bow shock (400 km/s assumed in this case). This gives a peak value of 132 nT. To test the sensitivity of the calculated Dst profile to the value chosen for $B2$, we bracket the Owens and Cargill empirical value (132 nT) with a lower limit (66 nT) and an upper limit (217 nT). The lower limit corresponds to the merging value in Fig. 2, and was obtained with the Crooker et al. (1982) formula mentioned earlier. The upper limit is the stagnation field strength for this case.

To calculate Dst, we use the Burton–McPherron–Russell formula (Burton et al., 1975) as modified by O'Brien and McPherron (2000). This formula relates the time rate of change of Dst to the interplanetary electric field (E), solar wind dynamic pressure (P), and the decay rate of the ring current (τ).

$$\mathrm{dDst}/\mathrm{d}t = -\alpha\, E\ (\text{mV/m}) + b\, P^{1/2} - \text{Dst(nT)}/\tau(\text{h})\ \text{nT/h}, \quad (5)$$

where $\alpha = 4.5$ nT/h/(mV/m), b, as specified by McPherron and O'Brien (2001), is a function of E, which varies from ~12 nT/nPa$^{1/2}$ for small E to ~2 nT/nPa$^{1/2}$ for large E, and τ, as specified by O'Brien and McPherron (2000), is a function of E, which varies from ~19 h for very small E to ~2 h for very large E. The value of E in (5) is the rectified (i.e., zero if negative) GSM y-component of the motional electric field ($-\mathbf{V}\times\mathbf{B}$).

4. Phase 1 of the storm: The ICME-sheath

Following Tsurutani et al. (2003), we interpret the high point in the Bombay magnetogram at 9 h local time as indicating that the shock had arrived at this time (despite the

beginning of a rise at the previous hour). The shock transit time (from flare to arrival) was, therefore, about 16 h 40 min, based on the flare time being 11 h 20 min on September 1 Greenwich time (Carrington, 1860) and a 5 h time difference between the local times of Greenwich and Bombay (although the time difference based on the current international time zones is 5 h 30 min).

Based on a 16 h 40 min transit time, the assumed ambient solar wind and IMF conditions, and the suite of formulas described in the last section, one can obtain time profiles of the electric field in earth's reference frame through the ICME-sheath for the chosen three values of $B2$, an upper limit (217 nT), Owens and Cargill empirical value (132 nT), and a lower limit (66 nT). Substituting the electric field profiles thus obtained into Eq. (5) for Dst (assuming that the electric field was zero but the dynamic pressure remained the same after the passage of the ICME-pause when the presumed-northward phase of the ICME body passed over the earth) gives the Dst profiles shown in Fig. 4 superimposed on the reconstructed Bombay Dst profile of Fig. 1.

We suggest (as other have for different reasons) that the figure might retrieve the 1859 storm from the realm of unique mutant monstrosities – a singularity in a class by itself – and place it instead in the regular population of magnetic storms arranged as the end member in order of strength. The suggestion is supported by the procedure, often adopted when faced with data containing suspicious outliers, of discarding the extreme point. Then, one is left with a maximum negative H excursion (~ -1200 nT), which is still well below any measured Dst, but which gives an hourly average of ~ -625 nT. This value lies just below the tip of the middle, calculated Dst curve for $B2 = 132$ nT and suggests that the middle calculated curve might represent the actual Dst for the 1859 storm better than either the Bombay magnetogram as originally interpreted or the extreme calculated Dst in Fig. 4 based on the stagnation field strength. Two other factors argue for this conservative, greatest-but-still-regular classification of the Carrington storm. First, the middle curve in Fig. 3 is the a priori expectation for this storm based on models

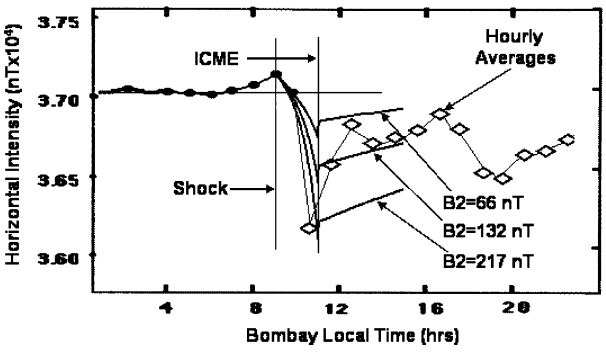

Fig. 4. Dst calculated from the E field and ram pressure throughout the ICME-sheath modeled as described in the text and using the Burton et al. formula (Eq. (5)) with the O'Brien and McPherron (2000) specification of the decay time as a function of E and the McPherron and O'Brien (2001) specification of the pressure coefficient as a function of E.

obtained by empirical fitting to other ICME storms. Second, the recovery phase calculated for the middle curve fits most of the observed recovery fairly well.

We turn now to comment briefly on the second phase of the storm, the main phase of which occurred from 17:00 to 19:00 h on Sept. 2nd. This, too, was a major storm. As inferred directly from the Bombay magnetogram, Dst dropped about 500 nT. Since unlike the earlier main phase this one lies within the range of known storms, no mystery needing to be resolved is present here. Its relevance to the present discussion is that it clearly calls for incorporation into the whole storm scenario – two large main phases separated by a recovery phase. To us the simplest explanation of this sequence of events is the one we stated earlier, that both storms were caused by a single structure of which there many known examples, namely, a geoeffective ICME-sheath pushed earthward by a magnetic cloud across which the IMF rotated from northward to southward. What distinguishes this example of the south-north-south ICME complex is that the independent parameters that manifest storms combined to maximize the storm effect: speed of the ICME, southward IMF in the sheath, and a direct hit on the earth. Had the cloud been of the first-south-then-north type, the effect could have been more severe.

5. Loose ends and implications

It is, of course, unjustified to assume that just because we have managed to construct an interpretation of the Bombay magnetogram that allows it to be seen as having been produced by a regular (albeit extreme) storm (instead of a one-of-a-kind storm) that the interpretation is therefore necessary. We have shown only that such an interpretation is possible but not that it is unavoidable since many parameters had to be assumed, and although we justified our assumptions, the range of physically allowed alternatives is large. For example, we assumed that the solar wind ram pressure was continuous across the ICME-pause, which implies that the density was continuous. This is a reasonable a priori assumption since we took the density in the ICME-sheath to be $20/\text{cm}^3$ and the density in average ICME clouds is about $11/\text{cm}^3$ (Lepping et al., 2003) and here we have an exceptional cloud for which the density could have been twice the average. As a result of the assumption that the ram pressure was continuous across the ICME-pause the calculated Dst increased discontinuously there because E dropped to zero, which increased the pressure coefficient, b, discontinuously. Thus, although the ram pressure was constant, the ram pressure contribution to Dst increased. We could have increased the size of the jump more, and so have obtained a better fit to the recovery phase, by choosing a larger density in the ICME body, as did Li et al. (2005) to fit the full recovery of H from -1600 nT (which in their case required an implausibly large density discontinuity).

Apropos of uncertain ram pressure effects, according to Vasyliunas et al. (1982), if the driving term in the Burton

et al. equation (5) is interpreted as giving the rate of energy input to the ring current then it should be multiplied by the one-sixth power of ram pressure. If, following this directive, we redo the calculations with the pressure factor (normalized to the climatological value 1.34 nPa) included in the driving term, the drop in Dst approximately doubles. Indeed, Li et al. (2005) state that it is the existence of a ram-pressure factor in the driving term of the Temerin and Li (2002) model that allows them to fit the full H depression in the Bombay magnetogram. But, since none of the empirical parameters that have been determined for the Burton equation and its enhancement take this pressure factor into account, one cannot justifiably simply include it at this stage. The safer approach is to use the equations as they have been derived and tuned, which is what we have done. Finally to this list of reasons to keep an open mind regarding the meaning of the Bombay magnetogram despite our conservative interpretation of it, we add the fact that to arrive at our interpretation we used the O'Brien–McPherron enhanced Burton et al. equation beyond its tested range of validity.

All of this leads to interesting implications. The issue regarding the Bombay magnetogram for the 1859 storm is whether its unprecedented negative excursion resulted from ionospheric currents or magnetospheric currents. If it resulted from ionospheric currents, then the size of the excursion is not so exceptional, but the fact that ionospheric currents could profoundly affect a magnetogram at such low latitude remains an exceptional aspect of the storm. Such an interpretation would seem to imply that overhead auroras might have reached the latitude of Bombay, yet against this inference Green and Boardsen (2005) report that auroral records for the storm indicate that overhead auroras came no closer to Bombay than 10° latitude. If instead of ionospheric currents the deep negative excursion in the Bombay magnetogram resulted from magnetospheric currents, then we learn that in the case of super-storms the hourly averaged Dst index could be under-representing the actual extent of H-depression that we normally associate with the ring current. It would be interesting to recalculate the Dst of super-storms with higher cadence to see whether the real main phase excursion has been seriously truncated, in effect, by low-pass filtering.

Another lesson from the exercise is that the empirical coefficients that enter the enhanced Burton et al. equation should be recalculated with one-sixth power of ram pressure multiplying the driver term. Without recalculating the coefficients, this factor has the potential of changing the result by a factor of 2 for super-storms.

6. Summary and conclusions

- Taking hourly averages of the Bombay magnetogram gives a proxy for Dst in which the maximum negative H excursion is 850 nT instead of 1600 nT as in the unaveraged magnetogram. The local time of Bombay at the peak of the storm happens, by coincidence, to lie close to one of the local-time null points in the disturbance field asymmetry as determined from nine recent major magnetic storms, which means that as far as the asymmetry is concerned, the Bombay magnetogram is a reasonable proxy for Dst.
- The Bombay magnetogram exhibits two major H-depressions, which we interpret to mean that the event was caused by a geoeffective ICME-sheath followed by a magnetic cloud across which the magnetic field rotated from north to south. The first depression reached the extraordinary −1600 nT value. The second depression, although also large, was not outside of precedents for Dst.
- Using empirical formulas that relate the measured shock transit time to the ICME speed and peak field strength at 1 AU together with standard assumptions to specify preshock interplanetary conditions, we have constructed a model of geoeffective parameters throughout the ICME-sheath.
- With these as input to the Burton et al. equation for Dst as modified by O'Brien and McPherron, we have calculated three Dst profiles representing upper and lower limits bracketing an empirical a priori best case.
- The upper limit Dst profile lies reasonably close to hourly averaged Bombay magnetogram. If one discards the most extreme outlier of the Bombay measurements, the empirical best case Dst profile lies reasonably close to most of the hourly averaged Bombay magnetogram.
- It seems to be possible, therefore, to interpret the Bombay magnetogram as having been produced by magnetospheric currents instead of by ionospheric currents.
- There are interesting implications of this conclusion, one of which is that the hourly averaged Dst index might under-represent storm-time H-depressions during the main phase of super-storms.

Acknowledgment

This work was supported in part by the National Science Foundation under Grant ATM-0220396.

References

Akasofu, S.-I., Chapman, S. The lower limit of latitude (U.S. sector) of quiet auroral arcs, and its relation to Dst (H). Journal of Atmospheric and Terrestrial Physics 25, 9, 1963.

Bothmer, V., Rust, D.M. The field configuration of magnetic clouds and the solar cycle. in: Crooker, N.U., Joselyn, J.A., Feynman, J. (Eds.), Coronal Mass Ejections, Geophys. Monogr. Ser., vol. 99. AGU, Washington, DC, pp. 137–146, 1997.

Burton, R.K., McPherron, R.L., Russell, C.T. An empirical relationship between interplanetary conditions and Dst. Journal of Geophysical Research 80, 4204–4214, 1975.

Carrington, R.C. Description of a singular appearance seen in the sun on September 1, 1859. Monthly Notices of the Royal Astronomical Society 20, 13–15, 1860.

Cliver, E.W., Feynman, J., Garrett, H.B. An estimate of the maximum speed of the solar wind, 1938–1989. Journal of Geophysical Research 95, 17103–17112, 1990.

Cliver, E.W., Crooker, N.U., Cane, H.V. The semiannual variation of great geomagnetic storms: solar sources of great storms. in: Fischer, S., Vandas, M. (Eds.), Proceedings of First Soltip Symposium. Astronomical Institute of Czechoslovak Academy of Sciences, Prague, pp. 88–97, 1992.

Crooker, N.U., Siscoe, G.L., Russell, C.T., Smith, E.J. Magnetic field compression at the dayside magnetopause. Journal of Geophysical Research 87, 10407–10412, 1982.

Green, J.L., Boardsen, S. Duration and extent of the great auroral storm of 1859. Adv. Space Res. 38, 130–135, 2006.

Kamide, Y., Yokoyama, N., Gonzalez, W., Tsurutani, B.T., Daglis, I.A., Brekke, A., Masuda, S. Journal of Geophysical Research 103, 6917–6921, 1998.

Lees, L. Interaction between the solar plasma wind and the geomagnetic cavity. AIAA Journal 2, 1576–1582, 1964.

Lepping, R.P., Berdichevsky, D.B., Szabo, A., Arqueros, C., Lazarus, A.J. Profile of an average magnetic cloud at 1 AU for the quiet solar phase: wind observations. Solar Physics 212, 425–444, 2003.

Li, X., Temerin, M., Tsurutani, B.T., Alex, S. Modeling the 1–2 September 1859 super magnetic storm. Adv. Space Res. 38, 273–279, 2006.

Loomis, E. The great auroral exhibition of Aug. 28th to Sept. 4th, 1859. – 4th Article. American Journal of Science 79, 386–399, 1860.

Loomis, E. The aurora borealis, or polar light: its phenomena and its laws. in: Annual Report of the Board of Regents of the Smithsonian Institution for 1865. Government Printing Office, Washington, pp. 208–248, 1866.

McPherron, R.L., O'Brien, P. Predicting geomagnetic activity: the Dst index. in: Song, P. et al. (Eds.), Space Weather, Geophysical Monograph 125. American Geophysical Union, Washington, DC, pp. 339–346, 2001.

Mulligan, T., Russell, C.T., Luhmann, J.G. Solar cycle evolution of the structure of magnetic clouds in the inner heliosphere. Geophysical Research Letters 25, 2959–2963, 1998.

O'Brien, T.P., McPherron, R.L. An empirical phase space analysis of ring current dynamics: solar wind control of injection and decay. Journal of Geophysical Research 105, 7707–7719, 2000.

Owens, M., Cargill, P. Predictions of the arrival time of coronal mass ejections at 1 AU: an analysis of the causes of error. Annals of Geophysics 22, 661–671, 2004.

Silverman, S.M. Low latitude auroras prior to 1200 C.E. and Ezekiel's vision, this issue, doi:10.1016/j.asr.2005.03.158, 2005.

Siscoe, G.L. A quasi-self-consistent axially symmetric model for the growth of a ring current through earthward motion from a pre-storm configuration. Planetary and Space Science 27, 285–295, 1979.

Siscoe, G.L., Crooker, N.U., Erickson, G.M., Sonnerup, B.U.Ö, Schoendorf, J.A., Maynard, N.C., Siebert, K.D., Weimer, D.R., Wilson, G.R., White, W.W. MHD properties of magnetosheath flow. Planetary and Space Science 50, 461–471, 2002.

Temerin, M., Li, X. A new model for the prediction of Dst on the basis of the solar wind. Journal of Geophysical Research 107 (A12), SMP 31-1, 2002. CiteID 1472. doi:10.1029/2001JA007532.

Tsurutani, B.T., Gonzalez, W.D., Lakhina, G.S., Alex, S., 2003. The extreme magnetic storm of 1–2 September 1859. Journal of Geophysical Research 108 (A7), SSH 1-1, CiteID 1268. doi:10.1029/2002JA009504.

Vasyliunas, V.M., Kan, J.R., Siscoe, G.L., Akasofu, S.-I. Scaling relations governing magnetospheric energy transfer. Planetary and Space Science 30, 359–365, 1982.

White, W.W., Schoendorf, J.A., Siebert, K.D., Maynard, N.C., Weimer, D.R., Wilson, G.L., Sonnerup, B.U.Ö, Siscoe, G.L., Erickson, G.M. MHD simulation of magnetospheric transport at the mesoscale. in: Song, P., Singer, H.J., Siscoe, G.L. (Eds.), Space Weather, Geophysical Monograph 125. American Geophysical Union, Washington, DC, pp. 229–240, 2001.